Journal of Physics:
Condensed Matter

PURPOSE-LED PUBLISHING™

PAPER • **OPEN ACCESS**

Transfer learning from Hermitian to non-Hermitian quantum many-body physics

To cite this article: Sharareh Sayyad and Jose L Lado 2024 *J. Phys.: Condens. Matter* **36** 185603

View the article online for updates and enhancements.

You may also like

- Effects of non-heating users in heating residential buildings on heat consumption
X Y Gao, C L Tang, X Z Meng et al.
- Recent advances in non-fullerene organic photovoltaics enabled by green solvent processing
Shilin Li, Hong Zhang, Shengli Yue et al.
- Unitarity of the time-evolution and observability of non-Hermitian Hamiltonians for time-dependent Dyson maps
F S Luiz, M A de Ponte and M H Y Moussa

This content was downloaded from IP address 188.119.27.68 on 20/05/2025 at 19:02

OPEN ACCESS
IOP Publishing
Journal of Physics: Condensed Matter
J. Phys.: Condens. Matter **36** (2024) 185603 (8pp)
https://doi.org/10.1088/1361-648X/ad22f8

Transfer learning from Hermitian to non-Hermitian quantum many-body physics

Sharareh Sayyad[1] **and Jose L Lado**[2,*]

[1] Max Planck Institute for the Science of Light, Staudtstraße 2, 91058 Erlangen, Germany
[2] Department of Applied Physics, Aalto University, FI-00076 Aalto, Espoo, Finland

E-mail: jose.lado@aalto.fi

Received 7 December 2023, revised 8 January 2024
Accepted for publication 26 January 2024
Published 7 February 2024

Abstract

Identifying phase boundaries of interacting systems is one of the key steps to understanding quantum many-body models. The development of various numerical and analytical methods has allowed exploring the phase diagrams of many Hermitian interacting systems. However, numerical challenges and scarcity of analytical solutions hinder obtaining phase boundaries in non-Hermitian many-body models. Recent machine learning methods have emerged as a potential strategy to learn phase boundaries from various observables without having access to the full many-body wavefunction. Here, we show that a machine learning methodology trained solely on Hermitian correlation functions allows identifying phase boundaries of non-Hermitian interacting models. These results demonstrate that Hermitian machine learning algorithms can be redeployed to non-Hermitian models without requiring further training to reveal non-Hermitian phase diagrams. Our findings establish transfer learning as a versatile strategy to leverage Hermitian physics to machine learning non-Hermitian phenomena.

Supplementary material for this article is available online

Keywords: machine learning quantum matter, non-Hermitian physics, topological states

1. Introduction

The interplay between various degrees of freedom in many-body systems results in the emergence of novel phases of matter, including superconducting [1–6], Mott insulating [7–11], nematic [12–16] and topological [17–22] phases. Due to their inherent complexity, these systems are often studied computationally, using, e.g. quantum Monte Carlo methods [23–25] and tensor network approaches [26–28]. In recent years, machine learning methods [29, 30] have provided a complementary strategy to rationalize phases of matter, often in combination with conventional quantum many-body methods. The demonstrations of these roles played by machine learning methods in tackling many-body problems results in characterizing different phases of matter [31–40], deep learning of the quantum dynamics [41–44], obtaining many-body wave functions [45–49], and optimizing the performance of computational simulations [50].

Exploring correlated physics in open quantum systems attracts great interest mainly because of the systematic treatment of loss and gain in these systems, which quantitatively reproduces experimental observations [51–55]. In recent years, along with brute force studies of open quantum systems, understanding their effective descriptions based on non-Hermitian physics get momentum [56–61]. The studies of

* Author to whom any correspondence should be addressed.

Original Content from this work may be used under the terms of the Creative Commons Attribution 4.0 licence. Any further distribution of this work must maintain attribution to the author(s) and the title of the work, journal citation and DOI.

© 2024 The Author(s). Published by IOP Publishing Ltd

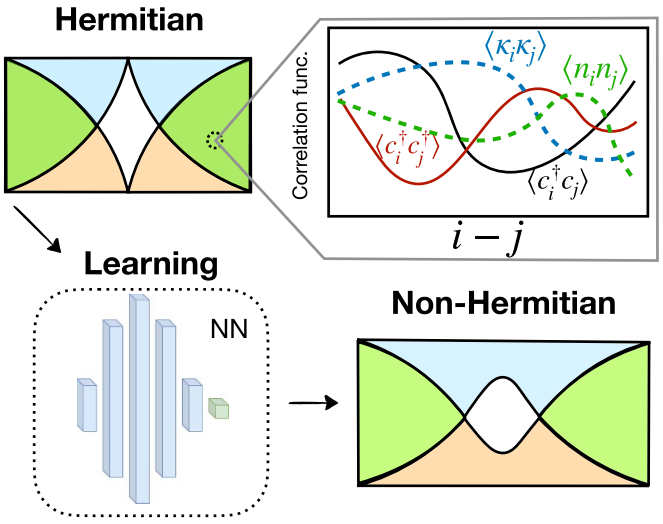


Figure 1. Non-Hermitian transfer learning: schematic illustration of the transfer learning methodology from Hermitian models to non-Hermitian physics. As an input, for each point of the phase diagram of the Hermitian model, short-range two-point (solid lines) and four-point (dashed lines) correlation functions are computed (equations (4) and (5)). The generated correlators for Hermitian systems are used to train a machine learning architecture, which in turn allows predicting the phase diagram from short-range correlators of the non-Hermitian model. The machine learning methodology allows extracting quasi-degeneracies and correlation entropies from the short-range correlators of the non-Hermitian model.

non-Hermitian models have initially focused on single-particle models [62–80], and its extension to the fully interacting realm has also gained attention recently [81–97]. Aside from these case studies, unraveling the physics of interacting non-Hermitian systems remains an open challenge due to the scarcity of exactly solvable models, and as conventional (Hermitian) many-body methods cannot be directly applied to the non-Hermitian limit. Specifically, obtaining the phase boundaries, understanding the stability of certain phases against non-Hermiticity, and characterizing exotic phases with no Hermitian counterparts remain in general open problems. Similar to the realm of Hermitian physics, machine learning methods, and specifically supervised [98–101], unsupervised [101, 102], and graph-informed methods [103] allowed to identify various phases of non-Hermitian non-interacting systems. In these methodologies, the inputs to train learning models are collected from non-Hermitian noninteracting systems and are used to characterize non-Hermitian phase diagrams. As computational methods for Hermitian interacting models are numerically less demanding and more stable than their non-Hermitian counterparts, learning phase diagrams of non-Hermitian many-body systems from Hermitian correlated models would open up a promising strategy to leverage many-body methods developed for interacting Hermitian models.

In this manuscript, we show that machine learning methods purely trained on Hermitian many-body data can predict interacting regimes in non-Hermitian interacting models. For concreteness purposes, we explore the different regimes of the non-Hermitian dimerized Kitaev-Hubbard chain using machine learning techniques schematically shown in figure 1. Here, we collect various correlation functions, orders of quasi-degeneracies, and correlation entropies at different parameter regimes of the Hermitian limit of our model. Using this input, we demonstrate that non-Hermitian regime crossovers can be identified using a machine-learning methodology trained on short-range Hermitian correlation functions. The outcomes of these supervised learning schemes are degrees of quasi-degeneracies and correlation entropies, which can characterize various regimes of the non-Hermitian model. Our findings reveal that employing correlation entropy as a classifier allows characterizing all regimes of the system. Our machine-learning approach reliably learns various regimes that share similarities with the Hermitian model. Our method also successfully delineates the regime crossovers even when the correlation effect in the non-Hermitian interacting model deforms the Hermitian phase diagram.

2. Non-Hermitian interacting model

We focus on an interacting non-Hermitian model whose phase boundaries can be solved exactly in the thermodynamic limit [93]. The non-Hermitian dimerized Kitaev–Hubbard Hamiltonian on a chain with length L is given by

$$\mathcal{H} = -\sum_{j=1}^{L-1}\left[t_j\left(c_j^\dagger c_{j+1} + c_{j+1}^\dagger c_j\right) + \Delta_j\left(c_j^\dagger c_{j+1}^\dagger + c_{j+1}c_j\right)\right] + \sum_{j=1}^{L-1}\left(U_j - \mathrm{i}\delta_j\right)\left(2n_j - 1\right)\left(2n_{j+1} - 1\right), \quad (1)$$

where $c_j^\dagger$ (c_j) is a creation (annihilation) operator for spinless fermion at site j associated with the fermion density $n_j = c_j^\dagger c_j$. Here t_j, Δ_j, and $U_j - i\delta_j$ denote, respectively, real-valued dimerized hopping amplitude, superconducting pairing amplitude, and complex-valued Hubbard interaction strength. Considering the site-independent parameter $\mathcal{O} \in \{t, \Delta, U, \delta\}$, $\mathcal{O}_j \in \{t_j, \Delta_j, U_j, \delta_j\}$ for $1 \leqslant j \leqslant L$ reads $\mathcal{O}_j = \mathcal{O}(1-\eta)$ if $j \bmod 2 = 0$ and $\mathcal{O}_j = \mathcal{O}(1+\eta)$ if $j \bmod 2 = 1$, where η is the real-valued dimerization parameter.

The Hamiltonian in equation (1) is exactly solvable when $\Delta = t$. At this parameter regime, the interacting model can be mapped to a quadratic fermionic model upon successive two Jordan-Wigner transformations and a spin rotation [93]. Through this procedure, one can show that the spectrum of the effective quadratic Hamiltonian undergoes gap closure upon setting $\frac{U}{t} = \pm\sqrt{\left|\frac{\delta^2}{t^2} - \frac{(1\pm\eta)^2}{(1\mp\eta)^2}\right|}$, and $\frac{U}{t} = \pm\frac{1\pm\eta}{1\mp\eta}$. These relations ensure the closure of the real-line gaps and the appearance of zero degeneracies in the imaginary part of the spectrum, respectively. Note that these two equations coincide when the non-Hermiticity parameter vanishes, i.e. $\delta = 0$.

As $\mathcal{H}$ respects the charge conjugation symmetry, eigenvalues come in pairs such that the set of all energies satisfy $\{\varepsilon\} = \{\varepsilon^*\}$. This implies that degeneracies of phases can be merely obtained by vanishing real parts of the spectrum. In a finite system, finite size effects will give rise to small splitting between degenerate states in the thermodynamic limit.

For finite models, it is thus convenient to define the quasi-degeneracy χ given by

$$\chi = \sum_{\alpha} e^{-\lambda|\varepsilon_\alpha - \varepsilon_0|} \tag{2}$$

with ε_α being the αth eigenvalue, and ε_0 the ground state [104]. The parameter λ controls the energy resolution of the quasi-degeneracy, which in the limiting case $\lim_{\lambda\to\infty}\lim_{L\to\infty}\chi$ becomes the thermodynamic degeneracy of the ground state [105]. We will focus our analysis on system sizes with $L = 16$, that are large enough to show different transition regimes that would converge to the different phases of the model in the thermodynamic limit.

In addition to the quasi-degeneracy χ, we can characterize the phase boundaries using the electronic correlation entropy given by [34, 106–110]

$$\mathcal{C}_{\rm corr} = -\frac{1}{L}\sum_{j=1}^{L} s_j \log(s_j), \tag{3}$$

where $0 \leqslant s_j \leqslant 1$ is the jth eigenvalue of the correlation matrix. The elements of the correlation matrix $C^{\rm mat}$ are two-point correlation functions that read $C^{\rm mat}_{ij} = |\det[\sum_{ll'}^{[\chi]} \rho_{ij}^{ll'}]|$ with $\rho_{ij}^{ll'} = \langle\Psi_l|c_i^\dagger c_j|\Psi_{l'}\rangle$, where Ψ_l is the lth eigenstate on the ground state manifold, and $[\chi]$ is the closest integer to χ. The correlation matrix $\mathcal{C}_{\rm corr}$ measures many-body entanglement and vanishes in systems described by Hartree–Fock product states [34, 111–114]. It is worth noting that while superconducting states can be represented as a product state in the Nambu basis, the previous definition of correlation entropy yields a finite value for superconducting states. Large values of $\mathcal{C}_{\rm corr}$ in certain regions of the phase diagram imply that the system cannot be represented by a Hartree–Fock product state.

3. Machine learning methodology

We now present the machine learning methodology to learn the different regimes of the interacting models, taking as target functions χ and $\mathcal{C}_{\rm corr}$. The input of our machine-learning algorithm corresponds to short-range many-body correlators in the form of two-point and four-point correlation functions given by

$$d_{ij} = \langle c_i^\dagger c_j\rangle_{[\chi]}, \quad f_{ij} = \langle c_i^\dagger c_j^\dagger\rangle_{[\chi]}, \tag{4}$$

$$k_{ij} = \langle \kappa_{ij}\kappa_{ij}^\dagger\rangle_{[\chi]}, \quad p_{ij} = \langle n_i n_j\rangle_{[\chi]}, \tag{5}$$

where $\kappa_{ij} = c_i c_j$ and $\langle\hat{A}\rangle_{[\chi]} \equiv |\det[\sum_{ll'}^{[\chi]} A_{ll'}]|$ with $A_{ll'} = \langle\Psi_l|\hat{A}|\Psi_{l'}\rangle$. Here, i,j run on four neighboring sites in the middle of the chain so that the algorithm relies solely on short-range correlation functions. These correlation functions are used to predict the quasi-degeneracy χ and the correlation entropy $\mathcal{C}_{\rm corr}$. We collect 20 000 different non-Hermitian interacting realizations on the $(U/t,\eta)$ plane, taking the non-Hermiticity parameter as $\delta \in \{0, 0.5\}$. To predict the quasi-degeneracy, we explore two strategies, the first one is based on transforming the task in a classification problem for $[\chi]$, and the second one is a regression problem for χ. The prediction of $\mathcal{C}_{\rm corr}$ is treated as a regression problem. The details of our NN architecture for each of these cases are presented in the supplemental materials (SM) [115].

4. Results

We now present the predictions of different regimes based on various correlators for our Hermitian and non-Hermitian limits. We start with the Hermitian phase diagram shown in figures 2(a) and (b). These panels present the numerical regimes obtained with the exact diagonalization method [116]. The finite-size effect pushed the regime crossovers to smaller η values from the phase boundaries in the thermodynamic limit, a feature that can be systematically analyzed using finite size scaling [93]. Performing this scaling gives rise to the thermodynamic phase boundaries shown in the cyan lines [93].

The associated predicted regime crossovers using χ are displayed in figures 2 (c)–(f). Here, we compare the true (figures 2 (a) and (b) and predicted (figures 2(c)–(f)) phase diagrams obtained from training the NN model using the two-point correlation functions (figures 2(c) and (d)) or the combination of both two-point and four-point correlation functions (figures 2(e) and (f)). The values of $[\chi]$ in figures 2(a), (c) and (e) are discrete, and the predicted results belong to different classes of $[\chi]$. In panels figures 2(b),(d) and (f), a regression architecture is used to predict χ, and the predicted results figures 2(d) and (f) are obtained as a regression problem.

We now examine how the regimes of the non-Hermitian interacting model can be deduced from short-range correlators using a model trained by the Hermitian dataset with $\delta = 0.0$, as shown in figure 3. Figures 3(c)–(f) shows the predicted phase crossovers obtained by the algorithm trained with Hermitian data, which should be compared with true outputs of the non-Hermitian problem shown in figures 3(a) and (b). Interestingly, the predicted results based on two-point correlation functions based on a classification architecture for $[\chi]$ (figure 3(c)) display a large discrepancy. Such inaccurate prediction is eliminated by incorporating four-point correlation functions into the considered observables, as shown in figure 3(e). We further note that if we phrase the task as a regression problem, as shown in figures 3(b), (d) and (f), the predicted phase boundaries based on training with two-point correlation functions are more reliable, as shown in figure 3(d). These results show that the quasidegeneracy of the non-Hermitian model can be extracted from a model trained purely on Hermitian data.

Aside from χ, the different regimes can be characterized using the correlation entropy $\mathcal{C}_{\rm corr}$ both in Hermitian $\delta = 0$ and non-Hermitian $\delta = 0.5t$ systems as respectively shown in figures 4(a) and (b). Finite-size effects are reflected in the deviations from the cyan lines, which are inherited by the changes of $[\chi]$ that impact the definition of the correlation entropy. Interestingly, $\mathcal{C}_{\rm corr}$ exhibits further transitions, quantitatively

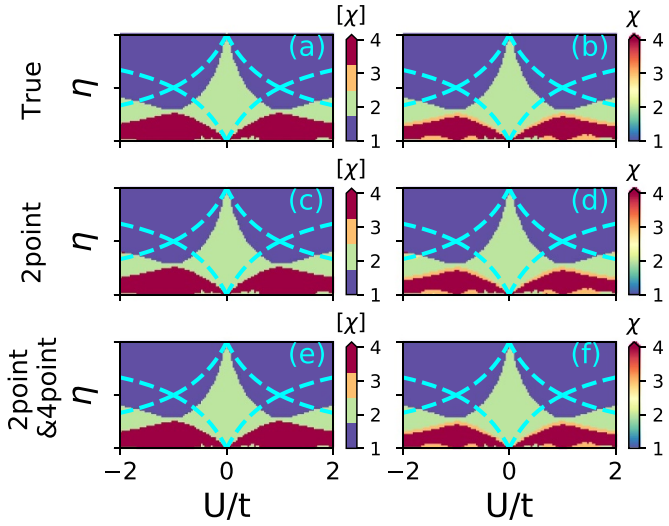


Figure 2. Hermitian interacting model: The phase diagram of the Hermitian many-body model with $L = 16$ on the $U/t - \eta$ plane at $\delta = 0.0$. The results in (a) and (b) are calculated by exact diagonalization. Panels (c), (d) use a machine learning architecture that uses solely two-point correlation functions as input. In contrast, panels (e), (f) use an architecture trained on both two-point and four-point correlation functions. The quasi-degeneracy in (c), (e) is treated as a discrete classifier for $[\chi]$, while it is treated as a regression problem in (d), (f). The boundaries in the thermodynamic limit are shown by cyan dashed lines.

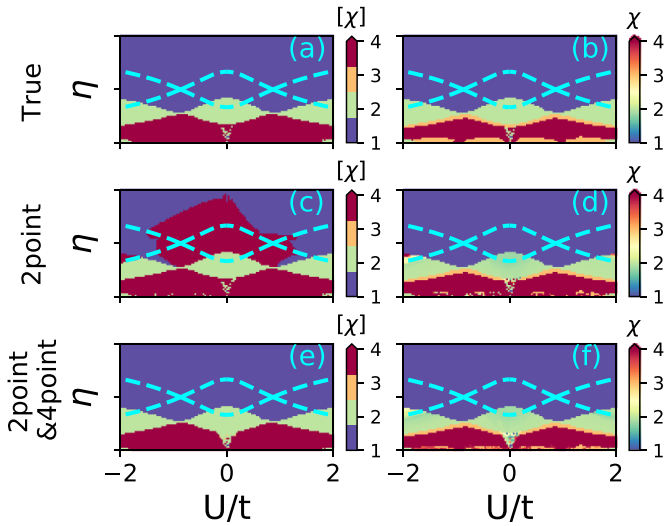


Figure 3. Non-Hermitian interacting model: the regimes of the non-Hermitian many-body model with $L = 16$ on the $U/t - \eta$ plane at $\delta = 0.5$. The results in (a) and (b) are calculated by exact diagonalization. The regimes in (c), (d) are obtained using architectures trained by two-point correlations, whereas (e), (f) are trained on both two-point and four-point correlation functions. The quasi-degeneracy in (c), (e) is treated as a discrete classifier for $[\chi]$, while it is treated as a regression problem in (d), (f). The boundaries in the thermodynamic limit are shown by cyan dashed lines and black dashed-dotted lines. It is observed that while two-point correlators fail to predict the non-Hermitian regimes in (c), the inclusion of four-point correlators recovers accurate regime crossovers (e).

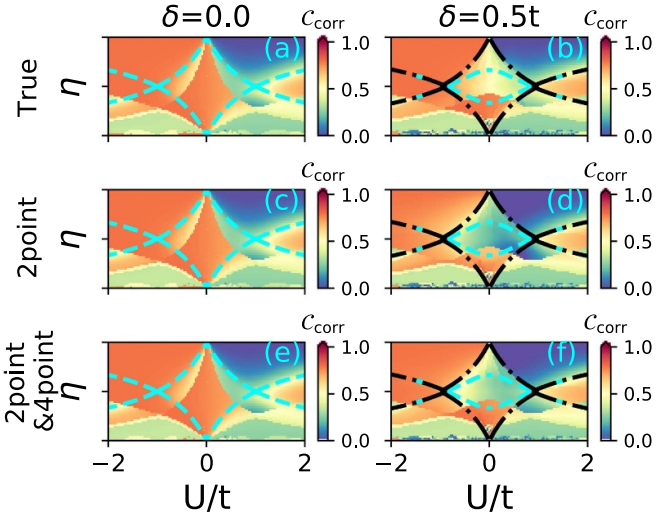


Figure 4. Correlation entropy predictions: the regimes of the non-Hermitian many-body model with $L = 16$ on the $U/t - \eta$ plane at $\delta = 0.0$ (a), (c), (e), $0.5t$ (b), (d), (f). The trained models are obtained using the Hermitian datasets with $\delta = 0.0$. The color bar denotes $\mathcal{C}_{\text{corr}}$. The regimes panels (c), (d) are obtained using the machine learning model trained by two-point correlation functions, whereas (e), (f) are trained on both two-point and four-point correlation functions. The boundaries in the thermodynamic limit given in the main text are shown by cyan dashed lines and black dashed-dotted lines.

described by the analytic phase boundaries. The absence of a finite size effect in different regions of the parameter space, delineated by the black dashed-dotted lines, signals the exponential convergence towards the ground state due to finite correlation gaps. Similar behavior is reported in Mott insulators [34, 117] and magnetic vortex liquids [118]. In figure 4, we present the various regimes for Hermitian (figures 4 (a), (c) and (e)) and non-Hermitian (figures 4(b), (d) and (f)) systems using a model trained on Hermitian models with only two-point (figures 4(c) and (d)) or the combination of two-point and four-point correlation functions (figures 4(e) and (f)). Overall, all the thermodynamic phase boundaries are qualitatively signaled by the correlation entropy. In the non-Hermitian cases, we can identify some regions, mainly inside the black diamond-like phase boundaries, featuring differences from the true results. These differences are reduced when including four-point correlation functions in the training of the Hermitian model; see also the SM [115]. It is worth noting that the regions with the most discrepancies have a topological superconducting nature, suggesting that phases with topological and many-body effects require higher-point correlation functions to be inferred with short-range information.

Our machine learning models trained only in Hermitian Hamiltonians can characterize the regimes of non-Hermitian interacting systems. Our results indicate that the model maintains its predictive accuracy across different parameter regions, showing the generalizability of our approach. It is

interesting to note that, while we observe a general agreement, small discrepancies between the machine learning predicted regimes and the computationally exact ones can be observed. This is because non-Hermitian many-body systems can show richer ground states than their Hermitian analog due to the extent of their spectrum in the complex plane. As a result, many-body wavefunctions in non-Hermitian models are genuinely different from their Hermitian counterparts, as these wavefunctions can span different regions of the Hilbert space beyond the original Hermitian training. Interestingly, this discrepancy opens the possibility of using our machine learning algorithms to directly identify non-Hermitian phases that do not have a Hermitian counterpart. Finding the smallest machine learning model to achieve our objective, developing a more interpretable algorithm [119, 120], and the possibility of domain adaptation from transfer learning [121, 122] are three potential future steps to enhance the performance of our algorithm. Pursuing domain adaptation would require fine-tuning the model with non-Hermitian data, which in turn requires actual knowledge of how the non-Hermitian phase diagram is. Our approach takes the perspective that no information about the non-Hermitian phase diagram is known, and only the Hermitian one is available for training. This approach emphasizes that even in the case in which no domain adaptation is done as in a situation in which no non-Hermitian data is available, a single shot transfer learning already provides valuable results. Our results provide a starting point for performing domain adaptation in non-Hermitian systems, and we hope that our manuscript will motivate further efforts in this direction.

5. Conclusion

To summarize, we have demonstrated a transfer machine learning methodology whereby training on Hermitian many-body models allows us to predict different regimes of interacting non-Hermitian quantum many-body models. Our algorithm effectively acts as a variational function that allows mapping the local correlators to the phase of the system. This opens the possibility of employing Hermitian many-body physics to understand the phase boundaries of non-Hermitian systems, leveraging solutions and methodologies currently only applicable to quantum many-body models. Our findings reveal that the prediction of quasi-degeneracy or correlation entropy allows the identification of different regions in interacting systems. Interestingly, these two methodologies are affected in a qualitatively different manner for finite-size effects, with the correlation entropy showing the fastest convergence to the thermodynamic limit. Our machine-learning methodology relies on short-range correlation functions, which open the possibility to potential deployments of our technique in experimental setups. Our results establish transfer learning as a promising strategy to map regimes on non-Hermitian quantum many-body models and to identify regimes featuring phenomena not observable in Hermitian models.

Data availability statement

All data that support the findings of this study are included within the article (and any supplementary files).

Acknowledgments

S S thanks F Marquardt for the helpful discussions. J L L acknowledges the computational resources provided by the Aalto Science-IT project, the financial support from the Academy of Finland Project Nos. 331342, 336243 and 349696, and the Jane and Aatos Erkko Foundation.

ORCID iDs

Sharareh Sayyad https://orcid.org/0000-0002-7725-7037
Jose L Lado https://orcid.org/0000-0002-9916-1589

References

[1] Dos Santos J M B L, Peres N M R and Neto A H C 2007 Graphene bilayer with a twist: electronic structure *Phys. Rev. Lett.* **99** 256802
[2] Proust C and Taillefer L 2019 The remarkable underlying ground states of cuprate superconductors *Annu. Rev. Condens. Matter Phys.* **10** 409–29
[3] Andrei E Y and MacDonald A H 2020 Graphene bilayers with a twist *Nat. Mater.* **19** 1265–75
[4] Sayyad S, Huang E W, Kitatani M, Vaezi M-S, Nussinov Z, Vaezi A and Aoki H 2020 Pairing and non-fermi liquid behavior in partially flat-band systems: beyond nesting physics *Phys. Rev.* B **101** 014501
[5] Nomura Y and Arita R 2022 Superconductivity in infinite-layer nickelates *Rep. Prog. Phys.* **85** 052501
[6] Kitatani M, Si L, Worm P, Tomczak J M, Arita R and Held K 2023 Optimizing superconductivity: from cuprates via nickelates to palladates *Phys. Rev. Lett.* **130** 166002
[7] Sayyad S and Eckstein M 2016 Slowdown of the electronic relaxation close to the Mott transition *Phys. Rev. Lett.* **117** 096403
[8] Seo K, Kotov V N and Uchoa B 2019 Ferromagnetic Mott state in twisted graphene bilayers at the magic angle *Phys. Rev. Lett.* **122** 246402
[9] Chatzieleftheriou M, Kowalski A, Berović M, Amaricci A, Capone M, De Leo L, Sangiovanni G and De'Medici L 2023 Mott quantum critical points at finite doping *Phys. Rev. Lett.* **130** 066401
[10] Kim S, Senthil T and Chowdhury D 2023 Continuous Mott transition in moiré semiconductors: role of long-wavelength inhomogeneities *Phys. Rev. Lett.* **130** 066301
[11] Tzeng Y-C, Chang P-Y and Yang M-F 2023 Interaction-induced metal to topological insulator transition *Phys. Rev.* B **107** 155106
[12] Fernandes R M, Chubukov A V and Schmalian J 2014 What drives nematic order in iron-based superconductors? *Nat. Phys.* **10** 97–104
[13] Samajdar R, Scheurer M S, Turkel S, Rubio-Verdú C, Pasupathy A N, Venderbos J W F and Fernandes R M 2021 Electric-field-tunable electronic nematic order in twisted double-bilayer graphene *2D Mater.* **8** 034005
[14] Sayyad S, Kitatani M, Vaezi A and Aoki H 2023 Nematicity-enhanced superconductivity in systems with a

non-fermi liquid behavior *J. Phys.: Condens. Matter* **35** 245605
[15] Mukasa K *et al* 2023 Enhanced superconducting pairing strength near a pure nematic quantum critical point *Phys. Rev.* X **13** 011032
[16] Jiang Q *et al* 2023 Nematic fluctuations in an orbital selective superconductor $Fe_{1+y}Te_{1-x}Se_x$ *Commun. Phys.* **6** 39
[17] Sheng D N, Gu Z-C, Sun K and Sheng L 2011 Fractional quantum Hall effect in the absence of landau levels *Nat. Commun.* **2** 389
[18] Neupert T, Santos L, Chamon C and Mudry C 2011 Fractional quantum Hall states at zero magnetic field *Phys. Rev. Lett.* **106** 236804
[19] Pollmann F, Berg E, Turner A M and Oshikawa M 2012 Symmetry protection of topological phases in one-dimensional quantum spin systems *Phys. Rev.* B **85** 075125
[20] Bauer B and Nayak C 2013 Area laws in a many-body localized state and its implications for topological order *J. Stat. Mech.* P09005
[21] Del Pozo F, Herviou L and Le Hur K 2023 Fractional topology in interacting one-dimensional superconductors *Phys. Rev.* B **107** 155134
[22] Kim S, Agarwala A and Chowdhury D 2023 Fractionalization and topology in amorphous electronic solids *Phys. Rev. Lett.* **130** 026202
[23] Troyer M and Wiese U-J 2005 Computational complexity and fundamental limitations to fermionic quantum Monte Carlo simulations *Phys. Rev. Lett.* **94** 170201
[24] Gezerlis A, Tews I, Epelbaum E, Gandolfi S, Hebeler K, Nogga A and Schwenk A 2013 Quantum Monte Carlo calculations with chiral effective field theory interactions *Phys. Rev. Lett.* **111** 032501
[25] Vaezi M-S, Negari A-R, Moharramipour A and Vaezi A 2021 Amelioration for the sign problem: an adiabatic quantum Monte Carlo algorithm *Phys. Rev. Lett.* **127** 217003
[26] Orús R 2014 A practical introduction to tensor networks: matrix product states and projected entangled pair states *Ann. Phys., NY* **349** 117–58
[27] Orús R 2019 Tensor networks for complex quantum systems *Nat. Rev. Phys.* **1** 538–50
[28] Cirac J I, Perez-Garcia D, Schuch N and Verstraete F 2021 Matrix product states and projected entangled pair states: concepts, symmetries, theorems *Rev. Mod. Phys.* **93** 045003
[29] Mehta P, Bukov M, Wang C-H, Day A G R, Richardson C, Fisher C K and Schwab D J 2019 A high-bias, low-variance introduction to machine learning for physicists *Phys. Rep.* **810** 1–124
[30] Carleo G, Cirac I, Cranmer K, Daudet L, Schuld M, Tishby N, Vogt-Maranto L and Zdeborová L 2019 Machine learning and the physical sciences *Rev. Mod. Phys.* **91** 045002
[31] Broecker P, Carrasquilla J, Melko R G and Trebst S 2017 Machine learning quantum phases of matter beyond the fermion sign problem *Sci. Rep.* **7** 1–10
[32] Rodriguez-Nieva J F and Scheurer M S 2019 Identifying topological order through unsupervised machine learning *Nat. Phys.* **15** 790–5
[33] Scheurer M S and Slager R-J 2020 Unsupervised machine learning and band topology *Phys. Rev. Lett.* **124** 226401
[34] Aikebaier F, Ojanen T and Lado J L 2023 Extracting electronic many-body correlations from local measurements with artificial neural networks *SciPost Phys. Core* **6** 030
[35] Van Nieuwenburg E P L, Liu Y-H and Huber S D 2017 Learning phase transitions by confusion *Nat. Phys.* **13** 435–9
[36] Koch R and Lado J L 2022 Designing quantum many-body matter with conditional generative adversarial networks *Phys. Rev. Res.* **4** 033223
[37] Liu Y-H and Van Nieuwenburg E P L 2018 Discriminative cooperative networks for detecting phase transitions *Phys. Rev. Lett.* **120** 176401
[38] Greplova E, Valenti A, Boschung G, Schäfer F, Lörch N and Huber S D 2020 Unsupervised identification of topological phase transitions using predictive models *New J. Phys.* **22** 045003
[39] Karjalainen N, Lippo Z, Chen G, Koch R, Fumega A O and Lado J L 2023 Hamiltonian inference from dynamical excitations in confined quantum magnets *Phys. Rev. Appl.* **20** 024054
[40] Tibaldi S, Magnifico G, Vodola D and Ercolessi E 2023 Unsupervised and supervised learning of interacting topological phases from single-particle correlation functions *SciPost Phys.* **14** 1–18
[41] Hartmann M J and Carleo G 2019 Neural-network approach to dissipative quantum many-body dynamics *Phys. Rev. Lett.* **122** 250502
[42] Van Nieuwenburg E, Bairey E and Refael G 2018 Learning phase transitions from dynamics *Phys. Rev.* B **98** 060301
[43] Reh M, Schmitt M and Gärttner M 2021 Time-dependent variational principle for open quantum systems with artificial neural networks *Phys. Rev. Lett.* **127** 230501
[44] Mohseni N, Fösel T, Guo L, Navarrete-Benlloch C and Marquardt F 2022 Deep learning of quantum many-body dynamics via random driving *Quantum* **6** 714
[45] Carleo G and Troyer M 2017 Solving the quantum many-body problem with artificial neural networks *Science* **355** 602–6
[46] Szabo A and Castelnovo C 2020 Neural network wave functions and the sign problem *Phys. Rev. Res.* **2** 033075
[47] Valenti A, Greplova E, Lindner N H and Huber S D 2022 Correlation-enhanced neural networks as interpretable variational quantum states *Phys. Rev. Res.* **4** L012010
[48] Glielmo A, Rath Y, Csanyi G, De Vita A and Booth G H 2020 Gaussian process states: a data-driven representation of quantum many-body physics *Phys. Rev.* X **10** 041026
[49] Reh M, Schmitt M and Gärttner M 2023 Optimizing design choices for neural quantum states *Phys. Rev.* B **107** 195115
[50] Czischek S, Gärttner M and Gasenzer T 2018 Quenches near ising quantum criticality as a challenge for artificial neural networks *Phys. Rev.* B **98** 024311
[51] Rotter I and Bird J P 2015 A review of progress in the physics of open quantum systems: theory and experiment *Rep. Prog. Phys.* **78** 114001
[52] Zhang J-W *et al* 2022 Dynamical control of quantum heat engines using exceptional points *Nat. Commun.* **13** 6225
[53] Perina Jr J, Miranowicz A, Chimczak G and Kowalewska-Kudlaszyk A 2022 Quantum Liouvillian exceptional and diabolical points for bosonic fields with quadratic Hamiltonians: the Heisenberg-Langevin equation approach *Quantum* **6** 883
[54] Bu J-T *et al* 2023 Enhancement of quantum heat engine by encircling a Liouvillian exceptional point *Phys. Rev. Lett.* **130** 110402
[55] Szankowski P 2023 Introduction to the theory of open quantum systems *SciPost Phys. Lect. Notes* 68
[56] Ashida Y, Gong Z and Ueda M 2020 Non-Hermitian physics *Adv. Phys.* **69** 249–435
[57] Bergholtz E J, Budich J C and Kunst F K 2021 Exceptional topology of non-Hermitian systems *Rev. Mod. Phys.* **93** 015005
[58] Maraviglia N *et al* 2022 Photonic quantum simulations of coupled $\mathcal{PT}$-symmetric Hamiltonians *Phys. Rev. Res.* **4** 013051

[59] Linpeng X, Bresque L, Maffei M, Jordan A N, Auffèves A and Murch K W 2022 Energetic cost of measurements using quantum, coherent and thermal light *Phys. Rev. Lett.* **128** 220506
[60] Banerjee A, Sarkar R, Dey S and Narayan A 2023 Non-Hermitian topological phases: principles and prospects *J. Phys.: Condens. Matter* **35** 333001
[61] Brzezicki W, Silveri M, Plodzien M, Massel F and Hyart T 2023 Non-Hermitian topological quantum states in a reservoir-engineered transmon chain *Phys. Rev.* B **107** 115146
[62] Joglekar Y N, Marathe R, Durganandini P and Pathak R K 2014 PT spectroscopy of the Rabi problem *Phys. Rev.* A **90** 040101
[63] Agarwal K S, Pathak R K and Joglekar Y N 2015 Exactly solvable PT-symmetric models in two dimensions *Europhys. Lett.* **112** 31003
[64] Agarwal K S, Pathak R K and Joglekar Y N 2018 Raising the PT transition threshold by strong coupling to neutral chains *Phys. Rev.* A **97** 042107
[65] Gong Z, Ashida Y, Kawabata K, Takasan K, Higashikawa S and Ueda M 2018 Topological phases of non-Hermitian systems *Phys. Rev.* X **8** 031079
[66] Kawabata K, Shiozaki K, Ueda M and Sato M 2019 Symmetry and topology in non-Hermitian physics *Phys. Rev.* X **9** 041015
[67] Li J, Harter A K, Liu J, de Melo L, Joglekar Y N and Luo L 2019 Observation of parity-time symmetry breaking transitions in a dissipative floquet system of ultracold atoms *Nat. Commun.* **10** 855
[68] Wang T, Fang J, Xie Z, Dong N, Joglekar Y N, Wang Z, Li J and Luo L 2020 Observation of two PT transitions in an electric circuit with balanced gain and loss *Eur. Phys. J.* D **74** 167
[69] Sayyad S, Yu J, Grushin A G and Sieberer L M 2021 Entanglement spectrum crossings reveal non-Hermitian dynamical topology *Phys. Rev. Res.* **3** 033022
[70] Chen W, Abbasi M, Joglekar Y N and Murch K W 2021 Quantum jumps in the non-Hermitian dynamics of a superconducting qubit *Phys. Rev. Lett.* **127** 140504
[71] Sayyad S and Kunst F K 2022 Realizing exceptional points of any order in the presence of symmetry *Phys. Rev. Res.* **4** 023130
[72] Chen W, Abbasi M, Ha B, Erdamar S, Joglekar Y N and Murch K W 2022 Decoherence-induced exceptional points in a dissipative superconducting qubit *Phys. Rev. Lett.* **128** 110402
[73] Abbasi M, Chen W, Naghiloo M, Joglekar Y N and Murch K W 2022 Topological quantum state control through exceptional-point proximity *Phys. Rev. Lett.* **128** 160401
[74] Sayyad S, Stalhammar M, Rodland L and Kunst F K 2022 Symmetry-protected exceptional and nodal points in non-Hermitian systems (arXiv:2204.13945)
[75] Kawabata K and Ueda M 2022 Nonlinear landauer formula: nonlinear response theory of disordered and topological materials *Phys. Rev.* B **106** 205104
[76] Sayyad S 2022 Protection of all nondefective twofold degeneracies by antiunitary symmetries in non-Hermitian systems *Phys. Rev. Res.* **4** 043213
[77] Xiao Z, Kawabata K, Luo X, Ohtsuki T and Shindou R 2022 Level statistics of real eigenvalues in non-Hermitian systems *Phys. Rev. Res.* **4** 043196
[78] Kawabata K, Numasawa T and Ryu S 2023 Entanglement phase transition induced by the non-Hermitian skin effect *Phys. Rev.* X **13** 021007
[79] Gal Y L, Turkeshi X and Schirò M 2023 Volume-to-area law entanglement transition in a non-Hermitian free fermionic chain *SciPost Phys.* **14** 138
[80] Turkeshi X and Schiró M 2023 Entanglement and correlation spreading in non-Hermitian spin chains *Phys. Rev.* B **107** L020403
[81] Fukui T and Kawakami N 1998 Breakdown of the Mott insulator: exact solution of an asymmetric Hubbard model *Phys. Rev.* B **58** 16051–6
[82] Buča B, Booker C, Medenjak M and Jaksch D 2020 Bethe ansatz approach for dissipation: exact solutions of quantum many-body dynamics under loss *New J. Phys.* **22** 123040
[83] Yamamoto K, Nakagawa M, Adachi K, Takasan K, Ueda M and Kawakami N 2019 Theory of non-Hermitian fermionic superfluidity with a complex-valued interaction *Phys. Rev. Lett.* **123** 123601
[84] Nakagawa M, Tsuji N, Kawakami N and Ueda M 2020 Dynamical sign reversal of magnetic correlations in dissipative Hubbard models *Phys. Rev. Lett.* **124** 147203
[85] Nakagawa M, Kawakami N and Ueda M 2021 Exact liouvillian spectrum of a one-dimensional dissipative Hubbard model *Phys. Rev. Lett.* **126** 110404
[86] Zhang X Z and Song Z 2021 η-pairing ground states in the non-Hermitian Hubbard model *Phys. Rev.* B **103** 235153
[87] Hyart T and Lado J L 2022 Non-Hermitian many-body topological excitations in interacting quantum dots *Phys. Rev. Res.* **4** L012006
[88] Yoshida H and Katsura H 2022 Exact analysis of the Liouvillian gap and dynamics in the dissipative SU(N) Fermi-Hubbard model pp 1–7 (arXiv:2209.03743)
[89] Yamamoto K, Nakagawa M, Tezuka M, Ueda M and Kawakami N 2022 universal properties of dissipative Tomonaga-luttinger liquids: Case study of a non-Hermitian XXZ spin chain *Phys. Rev.* B **105** 205125
[90] Wang Y-N, You W-L and Sun G 2022 Quantum criticality in interacting bosonic Kitaev-Hubbard models *Phys. Rev.* A **106** 053315
[91] Shen R and Lee C H 2022 Non-Hermitian skin clusters from strong interactions *Commun. Phys.* **5** 238
[92] Yamamoto K and Kawakami N 2023 universal description of dissipative Tomonaga-luttinger liquids with SU(n) spin symmetry: exact spectrum and critical exponents *Phys. Rev.* B **107** 045110
[93] Sayyad S and Lado J L 2023 Topological phase diagrams of exactly solvable non-Hermitian interacting Kitaev chains *Phys. Rev. Res.* **5** L022046
[94] Shen R, Chen T, Aliyu M M, Qin F, Zhong Y, Loh H and Lee C H 2023 Proposal for observing yang-lee criticality in rydberg atomic arrays *Phys. Rev. Lett.* **131** 080403
[95] Han S, Schultz D J and Kim Y B 2023 Complex fixed points of the non-Hermitian kondo model in a luttinger liquid (arXiv:2302.07883)
[96] Sayyad S 2023 Non-Hermitian chiral anomalies in interacting systems (arXiv:2306.14766)
[97] Ghosh S, Sengupta K and Paul I 2023 Hilbert space fragmentation imposed real spectrum of a non-Hermitian system (arXiv:2307.05679)
[98] Cheng Z and Yu Z 2021 Supervised machine learning topological states of one-dimensional non-Hermitian systems *Chin. Phys. Lett.* **38** 070302
[99] Zhang L-F, Tang L-Z, Huang Z-H, Zhang G-Q, Huang W and Zhang D-W 2021 Machine learning topological invariants of non-Hermitian systems *Phys. Rev.* A **103** 012419
[100] Narayan B and Narayan A 2021 Machine learning non-Hermitian topological phases *Phys. Rev.* B **103** 035413
[101] Ahmed W W, Farhat M, Staliunas K, Zhang X and Wu Y 2023 Machine learning for knowledge acquisition and accelerated inverse-design for non-Hermitian systems *Commun. Phys.* **6** 2

[102] Yu Y, Yu Li-W, Zhang W, Zhang H, Ouyang X, Liu Y, Deng D-L and Duan L-M 2022 Experimental unsupervised learning of non-Hermitian knotted phases with solid-state spins *npj Quantum Inf.* **8** 116
[103] Shang C *et al* 2022 Experimental identification of the second-order non-Hermitian skin effect with physics-graph-informed machine learning *Adv. Sci.* **9** 2202922
[104] For computational purposes, the previous sum can be restricted to a subset of the lowest lying states
[105] We take $1/\lambda(=0.005)$
[106] Gersdorf P, John W, Perdew J P and Ziesche P 1997 Correlation entropy of the hsub 2 molecule *Int. J. Quantum Chem.* **61** 935–41
[107] Huang Z, Wang H and Kais S 2006 Entanglement and electron correlation in quantum chemistry calculations *J. Mod. Opt.* **53** 2543–58
[108] Esquivel R O, Rodriguez A L, Sagar R P, Ho M and Smith V H 1996 Physical interpretation of information entropy: numerical evidence of the collins conjecture *Phys. Rev.* A **54** 259–65
[109] Benavides-Riveros C L, Lathiotakis N N, Schilling C and Marques M A L 2017 Relating correlation measures: the importance of the energy gap *Phys. Rev.* A **95** 032507
[110] Aikebaier F, Ojanen T and Lado J L 2023 Machine learning the Kondo entanglement cloud from local measurements (arXiv:2311.07253 [cond-mat.str-el])
[111] Siegbahn P E M, Almlöf J, Heiberg A and Roos B O 1981 The complete active space SCF (CASSCF) method in a newton–raphson formulation with application to the HNO molecule *J. Chem. Phys.* **74** 2384–96
[112] Debertolis M, Florens S and Snyman I 2021 Few-body nature of kondo correlated ground states *Phys. Rev.* B **103** 235166
[113] Snyman I 2023 The structure of quasiparticles in a local Fermi liquid (arXiv:2308.15576 [cond-mat.str-el])
[114] Vanhala T I and Ojanen T 2023 Complexity of fermionic states (arXiv:2306.07584 [quant-ph])
[115] The supplemental material includes details on the architecture of neural networks, details on comparing predicted and true phase diagrams and further details on predicting non-Hemritian phase diagrams using non-Hemritian dataset
[116] Numerical calculations are performed using the dmrgpy package (availabe at: https://github.com/joselado/dmrgpy
[117] Jeckelmann E 2003 Optical excitations in a one-dimensional Mott insulator *Phys. Rev.* B **67** 075106
[118] Chern Li E, Buessen F L and Kim Y B 2021 Classical magnetic vortex liquid and large thermal Hall conductivity in frustrated magnets with bond-dependent interactions *npj Quantum Mater.* **6** 33
[119] Zhang W, Wang L and Wang Z 2019 Interpretable machine learning study of the many-body localization transition in disordered quantum Ising spin chains *Phys. Rev.* B **99** 054208
[120] Flam-Shepherd D, Wu T C, Gu X, Cervera-Lierta A, Krenn M and Aspuru-Guzik A 2022 Learning interpretable representations of entanglement in quantum optics experiments using deep generative models *Nat. Mach. Intell.* **4** 544–54
[121] Zen R, My L, Tan R, Hébert F'eric, Gattobigio M, Miniatura C, Poletti D and Bressan S 2020 Transfer learning for scalability of neural-network quantum states *Phys. Rev.* E **101** 053301
[122] Liu H-Y, Sun T-P, Wu Y-C, Han Y-J and Guo G-P 2023 Mitigating barren plateaus with transfer-learning-inspired parameter initializations *New J. Phys.* **25** 013039